

DIFFUSIVE BURNING OF LIQUID FUELS IN OPEN TRAYS

By David Burgess, Alexander Strasser, and Joseph Grumer

U. S. Department of the Interior, Bureau of Mines
Explosives Research Laboratory
Pittsburgh, Pennsylvania

INTRODUCTION

An assessment of the hazards of a new liquid fuel requires an estimate of its liquid burning rate (i.e., linear regression rate of the liquid surface) during spill fires in open air. The best-known work on this subject is that of Blinov and Khudiakov (1) who reported on flames of several hydrocarbon blends contained in shallow trays. Their findings, as reviewed and interpreted by Hottel (3), suggest that the burning rate above large pools is determined by the rate of radiative feedback of the flame's heat of combustion to the pool of liquid. The important implication of this rate-controlling process is that burning rate should increase asymptotically to a maximum value at very large pool diameter; this maximum rate should not be much greater than with pools of moderate dimension, i.e., 1-2 meter diameter.

Some support was given to the picture advanced by Blinov and Khudiakov and by Hottel in an earlier paper from this Laboratory (2). The present paper gives additional corroborative evidence based on data for methanol, liquefied natural gas, liquid hydrogen, and two amine fuels as well as four typical hydrocarbons. The paper also describes the effects of fuel temperature and of wind on burning rate, discusses the special problem of cryogenic fuels, and suggests that burning rate may be predicted with some confidence from the heats of vaporization and combustion of the fuel.

EXPERIMENTAL

Materials

The liquid hydrogen was preconverted parahydrogen, supplied by the contractor.* Unsymmetrical dimethyl hydrazine (UDMH) used was specification grade "Dimazine" supplied by the Chlor-Alkali Division of Food Machinery and Chemical Corporation; and diethylenetriamine (DETA) was obtained as a technical grade product from the Carbide and Carbon Chemicals Company. Liquefied natural gas (LNG) was prepared by total condensation of the local pipeline product, boiling at -150°C ., cf. methane, b.p. -161.5°C . Reagent grade hexane and xylene, purified absolute methanol, and technical grade benzene were used as received from the Fisher Scientific Company and c.p. butane as obtained from the Matheson Company, Inc.

Procedures

Our burning rate tests followed generally the experimental conditions of Blinov and Khudiakov (1, 3). The noncryogenic fuels were burned in trays of 7-240 cm. diameter and about 8 cm. depth, particular attention being given to flush-filling of the trays at the smallest diameters. Liquid hydrogen was burned in

*See Acknowledgment.

stainless steel dewars of 7-33 cm. diameter and LNG in insulated trays or within a diked area which had been precooled with liquid nitrogen. Almost all tests were conducted out-of-doors in winds of less than 1 f.p.s. average velocity.

Radiation from the flames was measured with one or more Eppley thermopiles (CaF₂ windows) spaced around the flames in a horizontal plane and far enough from the flames for the inverse square law to apply. Two typical records appear in Figure 1. The radiant power of a flame was calculated on the assumption that radiation is emitted with spherical symmetry from the center of the fuel tray. The total thermal power was computed on the assumption that combustion is complete, neglecting soot formation, with CO₂, N₂, and H₂O vapor as products.

Burning rates were calculated by assuming that the instantaneous radiation level is proportional to the burning rate at the same point in time and that the area under the radiation record is proportional to the total volume of fuel consumed. Alternative methods were used for specific purposes: (1) The liquid surface level was monitored with a thermocouple and burning rate computed from the required addition rate of fuel to maintain the level constant. (2) Measured volumes of water-insoluble fuels were poured onto water and burned completely; several depths of fuel, for example 1, 2, and 5 cm., were burned to comprise each burning rate determination. (3) Small trays of up to 38 cm. diameter were supported on a balance so that fuel consumption was established intermittently by weight loss. It was found that convection currents were sufficiently different around a small elevated tray that burning rates were generally higher than those obtained with the tray on a broad flat surface.

RESULTS AND OBSERVATIONS

Burning Rate as a Function of Time

Typical behavior on ignition is for the burning rate to accelerate through a short "burning-in" period. In the case of benzene, the burning rate was found to reach its steady value at about the time when bubbles appeared on the liquid surface. This induction period was observed at all tray diameters and is illustrated in Figure 2; methanol, UDMH, and the cryogenic fuels H₂ and LNG provided exceptions by the absence of an induction period.

Methanol and benzene flames at the same pool diameter (7.5 cm.) and the same initial vapor pressure (40 mm.Hg) were snuffed out after short intervals of burning as shown in Table 1; heat required for fuel vaporization, column 3, was estimated from the weight loss during burning; heat retained in the liquid, column 4, was estimated from the average temperature rise; total heat transfer from flame to liquid, column 5, is almost time-independent, and by chance circumstance of the tray diameter, almost equal for the two fuels. The induction period for benzene occurs during the first two minutes while much of the transferred heat is being stored in the liquid phase. Burning rate is constant after the "burn-in."

Burning Rate as Function of Fuel Temperature

Several fuels were burned in small brine-jacketed trays for an estimate of the temperature coefficient of burning rate. Results with ethyl ether, absolute methanol, and 95 percent ethanol are given in Figure 3. The correlating lines conform closely to our expectation that burning rate should vary inversely with the fuel's sensible heat of vaporization.

Burning Rate as Function of Pool Diameter and Wind Velocity

Steady burning rates in the near-absence of wind at various diameters of fuel tray are plotted in Figure 4. The curves represent the empirical expression

$$v = v_{\infty} (1 - e^{-\kappa d}) \quad (1)$$

wherein v is the linear burning rate and d the tray diameter. Two points for each fuel (solid circles) were used to evaluate the constants κ and v_{∞} , which are listed in Table 2. Figure 5 presents data specifically for benzene, the points near the curve resulting from experiments under nearly wind-free conditions. The dashed line represents the extrapolated burning rate, v_{∞} , and the points near this line were obtained by burning benzene in various natural and artificial winds ranging up to 4 meters per second.

Values of v_{∞} for the nine fuels studied are given as ordinates in Figure 6. The correlating line has the form

$$v_{\infty} = 0.0076 \left(\frac{\text{net heat of combustion, } \Delta H_c}{\text{sensible heat of vaporization, } \Delta H_v} \right) \text{ cm./min.} \quad (2)$$

No correction was made for incompleteness of combustion which was particularly evident in the soot-forming benzene flames.

Radiation and Absorption Measurements

The radiative outputs of some gaseous diffusion flames are compared in Table 3 with the total heats of combustion involved. It was demonstrated at several burner diameters that the apparent percentage of heat radiated to the surroundings was independent of the flow rate of fuel supplied. The effect of wind was always to reduce the percentage of heat dissipated radiatively.

Radiative outputs at various diameters of liquid-supported flames are given in Table 4. The percentage of heat radiated in the largest scale test is combined with burning rate values to give the radiant output per unit area of the liquid surface shown in the final column of Table 2. Hazards arising from this radiation may be diminished somewhat through absorption of the flame radiations by atmospheric water. Some representative percentages of absorption at various lengths of optical path by water vapor, by fuel vapor, and by the liquid fuel are given in Table 5.

Special Behavior of Cryogenic Fuels

Unconverted liquid hydrogen was poured into a deep pyrex dewar (7.0 cm. diameter \times 45 cm. deep), the bottom 15 cm. of which was filled with paraffin at 25° C. The time-dependent vaporization rate is illustrated in Figure 7. The first 20 seconds represents the transfer period during which spattering occurred and the vaporization rate was somewhat uncertain. Thereafter, vaporization seemed to follow a curve given by

$$v \text{ (linear regression rate)} = Kt^{-1/2} \quad (3)$$

wherein K has a value consistent with the solution of the one-dimensional, time-dependent, heat transfer problem (5), and zero time represents the point at which the paraffin surface was apparently cooled to liquid hydrogen temperature. Similar results were obtained on spilling liquid nitrogen onto warm insulating materials within deep vessels. However, on spillage of the cryogenic liquids N_2 and LNG into shallow insulated trays the time-dependent "tail" corresponding to equation 3 could not be reproduced; as illustrated in Figure 8 the vaporization rate typically decays to a nearly time-independent value which is clearly affected by air currents across the tray.

The result of igniting a cryogenic fuel during the first seconds after spillage is shown in the upper curve (LNG) of Figure 1. Start of spilling is indicated by a pip on the radiation record labeled A. Ignition was accomplished 7 seconds later and the duration of the radiative flash was no more than 4 seconds. The shape

of the radiation record during the first 30 seconds was never found to resemble the vaporization rate curves of Figures 7 and 8. The lower curve of Figure 1 shows the comparable flash on igniting benzene followed by a typical "burning-in" period of 30-40 seconds encountered with liquid hydrocarbons at room temperature.

The burning rates reported here for liquid hydrogen are less reliable than for the conventional fuels since evaporative losses become very high when one attempts to flush-fill a container. The liquid was burned in stainless steel dewars of three diameters with fuel consumption as shown in Figure 9. Burning rates were obtained from the initial slopes of the curves in Figure 9 corrected for the heat losses of the dewars. The dashed line of the figure shows this heat loss to be about equal to the terminal burning rate as the liquid level approached the bottom of the dewar. Burning rates in such small diameter vessels, i.e., 7, 15, and 33 cm. diameter, are typically very much affected by such casual crosswinds as occurred during these particular tests.

Other Observations Relative to Rate Measurements

Figures 10 and 11 illustrate phenomena which were observed in large diameter flames and which could be simulated by benzene flames above small pyrex dishes. The underside views of Figure 10 show the distribution of soot through the vapor zone between flame and liquid surface. The density of soot is increased by increasing the radial draft with a chimney as in Figure 10b. Soot has also been observed under ethylene flames in open air (4). The shape of the flame in 10b is quite similar to that of a large flame in quiet air; the burning rate, plotted in Figure 5, is comparable to v_{∞} . Figure 10c shows the flame dislocated from the rim of the tray by an excessive draft. With rectangular trays this tearing of the flame occurred with winds of about 3-4 m./sec., although the critical velocity was sensitive to the configuration of the apparatus. The burning rate typically decreases at this point of incipient blowoff, but if premixing of fuel vapor and air occurs at a point of flame stabilization then a much hotter flame develops (note the bright zone in Figure 10c) and burning rates can exceed v_{∞} .

In Figure 10 the pyrex dish is set into the bench top so that the rim of the dish is 1/2-inch above the surrounding flat surface. The flame is then stabilized at the rim. In Figure 11 the rim of the dish is mounted flush with the surrounding surface and one observes the "creeping" of the flame as heavy fuel vapors diffuse outward along the surface against the radial inflow of air. This phenomenon was noted particularly with butane flames and brought about the discontinuance of measurements above 76 cm. diameter. Burning rates and radiation levels increased appreciably (>20 percent) during each period of this flame instability.

It was confirmed that linear burning rates increase at tray diameters below 5-10 cm., such rate values being omitted from Figure 4 to avoid confusion. Flames at very small diameter are simple laminar diffusion flames and heat transfer to the liquid is demonstrably an edge effect of no interest in large-scale experiments. For example, methanol burning in a 7.5 cm. diameter, water-jacketed brass tray was consumed at a rate of 3.8 cc./min.; when a concentric inner tray of 4.4 cm. diameter was added, this inner tray being left empty, there was no change in the consumption rate of fuel; when the inner tray had a diameter of 5.4 cm., the volumetric rate fell to 3.1 cc./min. Thus, the "edge" of interest in small methanol flames is an annulus of slightly greater width than 1 cm.

DISCUSSION

The Dominance of Radiative Heat Transfer

From their studies of hydrocarbon flames, Blinov and Khudiakov proposed that burning rates are controlled by heat flux from the hot zone to the liquid surface. This concept was put into semi-quantitative form by Hottel in his review of the Russian paper (3).

$$\frac{q}{\pi d^2/4} = k_1 \frac{T_F - T_B}{d} + k_2 (T_F - T_B) + \sigma T_F^4 \cdot F (1 - e^{-kd}) \quad (4)$$

(Heat flux = conductive + convective + radiative components)

wherein T_F is the flame temperature, T_B the liquid surface temperature, presumably the boiling point, k_1 and k_2 are conductive and convective coefficients, respectively, d the pool diameter, σ the Stefan-Boltzman constant, F a flame shape factor for radiation to the liquid, and k an opacity coefficient. On dividing both sides of equation 4 by the volumetric heat of vaporization, $\rho \Delta H_v$, and neglecting conductive and convective terms, one obtains

$$v = \frac{\sigma T_F^4 F}{\rho \Delta H_v} (1 - e^{-kd}). \quad (5)$$

Conductive heat transfer becomes negligible at large diameters by virtue of being an edge effect. If one assumes that the Blinov and Khudiakov burning rates at small diameter are completely conduction-controlled, then by equation 4 the contribution of conduction is less than our experimental uncertainty at all diameters represented in Figure 4. It is not so easy to dispose of convective transfer, especially with the slower-burning flames. We have noted a steep temperature gradient at the interface between liquid and vapor phases in both methanol and benzene flames. The presence of soot particles above the benzene pool as shown in Figure 10 is also suggestive of convection. The strong absorption of flame radiation by methanol vapor; Table 5, dictates that the flame stand very close to the liquid surface which again favors convection as the heat transfer mode. On the other hand, we can rule out convection with the faster-burning butane and hydrogen flames since there was no sharp rise in temperature as a thermocouple emerged from the liquid phase into the vapor zone. Assuming for the sake of further discussion that heat transfer in large trays is exclusively radiative, equation 1 becomes the empirical equivalent of equation 5. On this basis, the empirical constant κ of equation 1 may be identified with Hottel's opacity coefficient k , and our extrapolated burning rate, v_∞ , is given by

$$v_\infty = \frac{\sigma T_F^4 \cdot F}{\rho \Delta H_v}. \quad (6)$$

No precise explanation is offered for the simple correlation of data given by equation 2 and Figure 6. Qualitatively, the relationship is easy to understand. The reciprocal of $(\Delta H_c / \Delta H_v)$ is the fraction of the flame's heat that must be fed back to the liquid to maintain a steady rate of vaporization. The smaller this fraction, the taller the flame must be to limit the efficiency of heat transfer; but the height of a diffusion flame, other things being equal, is determined by the rate of fuel feed, i.e., the burning rate. The linearity of the curve in Figure 6, and the small degree of scatter of data, were unexpected.

Since equation 2 is expected to have some practical significance in predicting the relative hazards of fuels, it is important to list its limitations. The data involved only single-component fuels (the LNG used was more than 90 percent methane) burning in unvitiated air, under unusually calm atmospheric conditions and at one atmosphere pressure. We know from experiments with methanol that the effect of atmospheric humidity must be minor. It is particularly important to note that no fuel studied was a monopropellant and that decomposition flames could hardly conform to the heat transfer picture described above.

The Effect of Wind on Burning Rate

The effect of minor winds (Figure 5) may be rationalized on the basis of the three variables T_F , F , and k in equation 5. If the effect of the wind is only to move the flame around, then T_F and F could reasonably remain unchanged; but as the flame's hot zone is ruffled the opacity is visibly increased and the result of Figure 5 could arise from such an increase of k , the opacity coefficient, that e^{-kd} becomes negligibly small. The effects of wind and of large pool diameter should therefore be identical.

Some caution is necessary in applying this concept to practical problems. In the case of an idealized spill in which the liquid surface is flush with the surrounding terrain and there are no velocity gradients in the moving air, one would expect v_{∞} to be the highest attainable burning rate. At higher wind velocities than those of Figure 5 the flame begins to blow off. However if the fuel is contained behind a bluff body (consider for example a half-empty fuel tank) one may no longer be dealing with a diffusion flame but with a turbulent premixed flame in which T_F is hundreds of degrees higher than in diffusion flames. We have observed burning rates equal to twice v_{∞} under some such circumstances and know of no upper limit.

Special Problems with Cryogenic Fuels

The data for liquid hydrogen and for liquefied natural gas were made consistent with other data in Figures 4 and 6 by either minimizing or correcting for any heat flow from the warm surroundings. However, in actual spills with ignition occurring at or shortly after spillage, heat conducted from the ground may be the dominant factor in the fuel's rate of vaporization. For example, when hydrogen was spilled onto warm paraffin, Figure 7, about 7 cm. of the liquid depth was vaporized in chilling the paraffin surface; thereafter, the liquid regression rate still remained faster for several minutes than the liquid burning rate obtained with insulated pools (Figure 9). With typical soils, the thermal diffusivity is higher than with paraffin and a liquid depth of 20 cm. can well be dissipated within the first minute after spillage (5).

We have no radiation records for the initial flash on spilling a large depth of liquid hydrogen into an ignition source. The data that we do have pertains to LNG and Figure 1 is representative. The area under the initial spike is never comparable to the radiation expected from fuel vaporization curves. We can only suppose that a large fraction of the fuel vapor escapes unignited.

CONCLUSIONS

Due to the dependence of burning rate on radiative heat transfer from flame to liquid, the burning rate approaches a constant value with increasing pool diameter. This constant burning rate is proportional to the ratio of the net heat of combustion to the sensible heat of vaporization. Winds raise the burning rates of unshielded fires to approach the large diameter value unless the flame is disrupted. The radiative flux to the environment is about 20-40 percent of the heat of combustion.

ACKNOWLEDGMENTS

This research was supported in part by the Department of the Air Force, Wright Air Development Center (Delivery Order (33-616)58-5: Research on the Hazards Associated with the Large Scale Production and Handling of Liquid Hydrogen); Department of the Navy (Office of Naval Research, Bureau of Ships, Bureau of Yards and Docks, and Bureau of Weapons)(Contract No. NAonr 8-61: Hazards of Vapor Explosions Associated with New Liquid Propellants); and Conch International Methane Limited and Continental Oil Company (Contract No. 14-09-0050-2155: The Flammability of Methane).

LITERATURE CITED

1. Blinov, V. I., and Khudiakov, G. N., Certain Laws Governing the Diffusive Burning of Liquids. Acad. Nauk, USSR, Doklady, vol. 113, 1957, pp. 1094-98.
2. Burgess, D. S., Grumer, J., and Wolfhard, H. G., Burning Rates of Liquid Fuels in Large and Small Open Trays. First International Symposium on Fire Research, November 1959, in print.
3. Hottel, H. C., Review of reference 1. Fire Research Abstracts and Reviews, vol. 1, 1958, pp. 41-44.
4. Singer, J. M., and Grumer, J., Unpublished data, this Laboratory.
5. Zabetakis, M. G., and Burgess, D. S., Research on the Hazards Associated with the Production and Handling of Liquid Hydrogen. Bureau of Mines Report of Investigations 5707, 1961.

Table 1.--Heat transferred to liquid phase during short periods of burning.

Minutes burned	Grams burned	ΔH_v , cal.	ΔH_f , cal.	ΔH_t , cal.
<u>Methanol, 5° C., initial</u>				
1	3.8	1100	250	1400
2	7.5	2300	500	2800
3	11.3	3400	700	4100
4	15.0	4500	900	5400
5	18.0	5400	1050	6500
<u>Benzene, 9° C., initial</u>				
1	4.0	500	750	1300
2	11	1400	1250	2700
3	21	2600	1550	4200
4	31	3800	1700	5500
5	41	5000	1800	6800

Table 2.--Summary of computed values bearing on radiative hazards of fires.

Fuel	K , cm. ⁻¹	v_m , cm./sec.	Thermal output per unit liquid surface, kcal./cm. ² sec.	
			Total	Radiated
Hexane	0.019	0.73	5.1	2.0
Butane	.027	.79	5.1	1.4
Benzene	.026	.60	5.1	1.8
Xylene	.012	.58	5.0	-
Methanol	.046	.17	.64	.11
UDMH	.025	.38	2.2	.60
Hydrogen	(0.07)	(1.4)	(2.8)	(0.7)
LNG	.030	.66	3.2	.74

Table 3.--Radiation by gaseous diffusion flames.

Fuel	Burner diameter, cm.	$100 \times \frac{\text{Radiative output}}{\text{Thermal output}}$
Hydrogen	0.51	9.5
	.91	9.1
	1.9	9.7
	4.1	11.1
	8.4	15.6
	20.3	15.4
Butane	40.6	16.9
	0.51	21.5
	.91	25.3
	1.9	28.6
	4.1	28.5
	8.4	29.1
Methane	20.3	28.0
	40.6	29.9
	0.51	10.3
	.91	11.6
	1.9	16.0
	4.1	16.1
Natural gas (95% CH ₄)	8.4	14.7
	20.3	19.2
	40.6	23.2

Table 4.--Radiation by liquid-supported diffusion flames.

Fuel	Vessel diameter, cm.	$100 \times \frac{\text{Radiative output}}{\text{Thermal output}}$
Hydrogen	33	25
Butane	30	20
	46	21
	76	27
LNG	38	21
	76	23
Methanol	2.5	12
	5	14
	15	17
	122	17
Benzene	5	38
	46	35
	76	35
	122	36

Table 5.--Percentage of absorption of flame radiations in cells with CaF_2 windows.

Fuel	Absorbing medium, path length, temperature		
	Liquid fuel,	Fuel vapor,	Steam,
	0.3 cm., 30° C.	8.9 cm., 100° C.	8.9 cm., 165° C.
Methanol	100	27*	13
Hydrogen	-	0	33
UDMH	> 98	43	18
Hexane	71	-	< 6
Benzene	62	11	-

*38 percent absorbed over 18.4 cm. path.

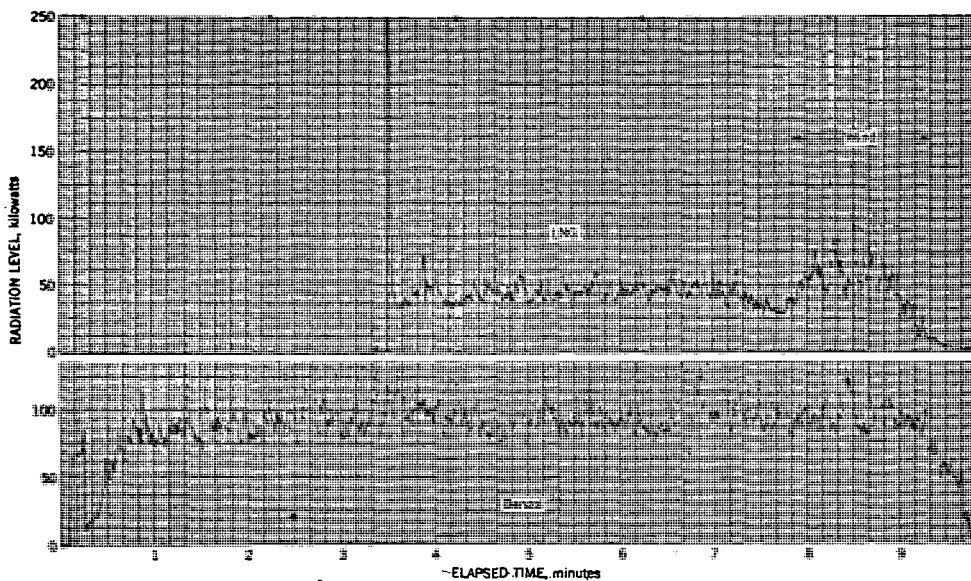


Figure 1.--Radiation Records on Burning about One Gallon (3640 cc.) of LNG and of Benzol in 15-inch Diameter Tray. LNG poured into warm tray at point A.

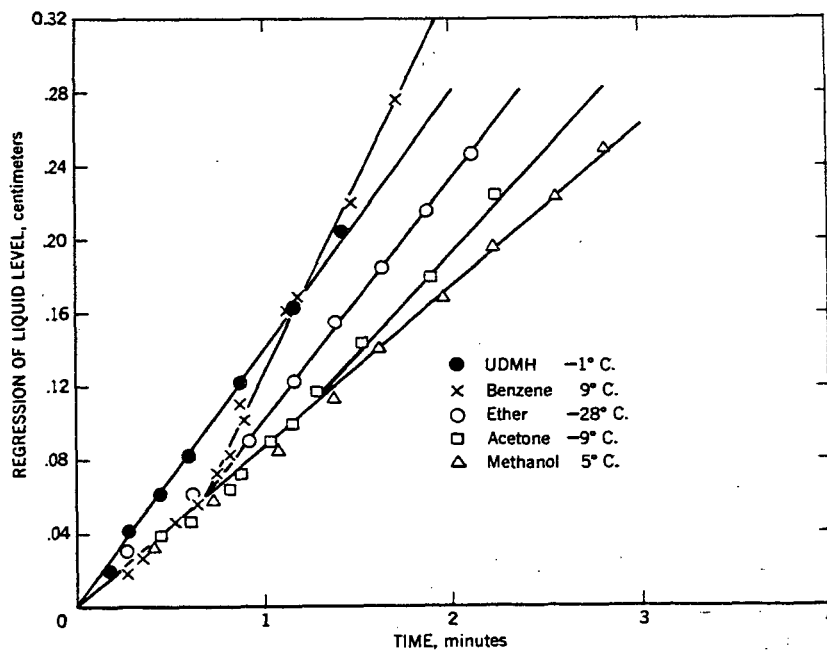


Figure 2.--Burning Rates of Five Liquid Fuels in a 3-inch Pyrex Vessel (3.5-inch for UDMH). Vapor Pressure 40 mm.Hg at Initial Liquid Temperature.

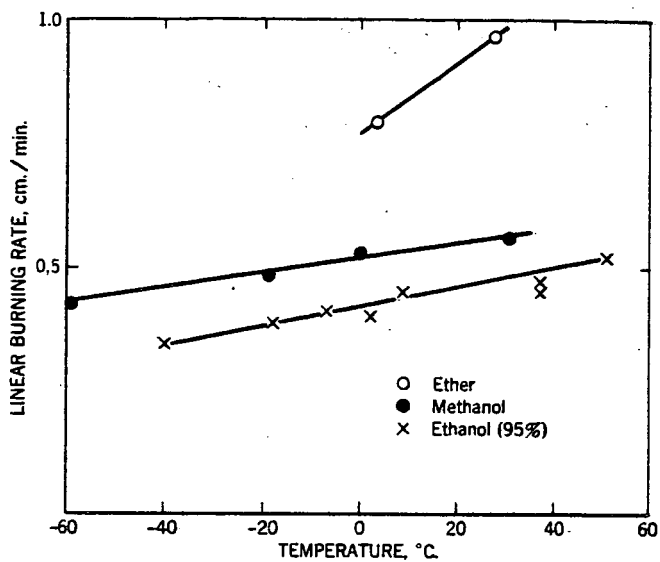


Figure 3.--Effect of Fuel Temperature on Steady Burning Rates in 7.5 cm. Diameter Brine-Jacketed Burner.

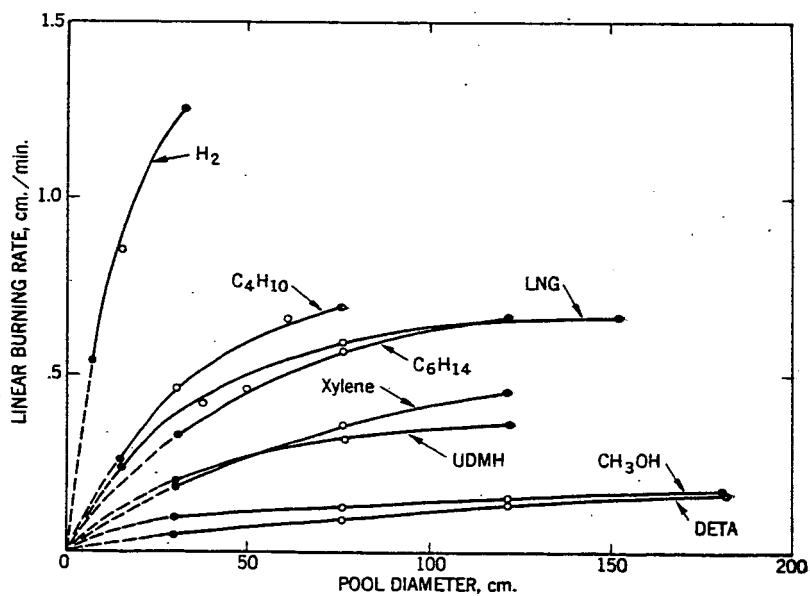


Figure 4.--Dependence of Liquid Burning Rate on Pool Diameter.

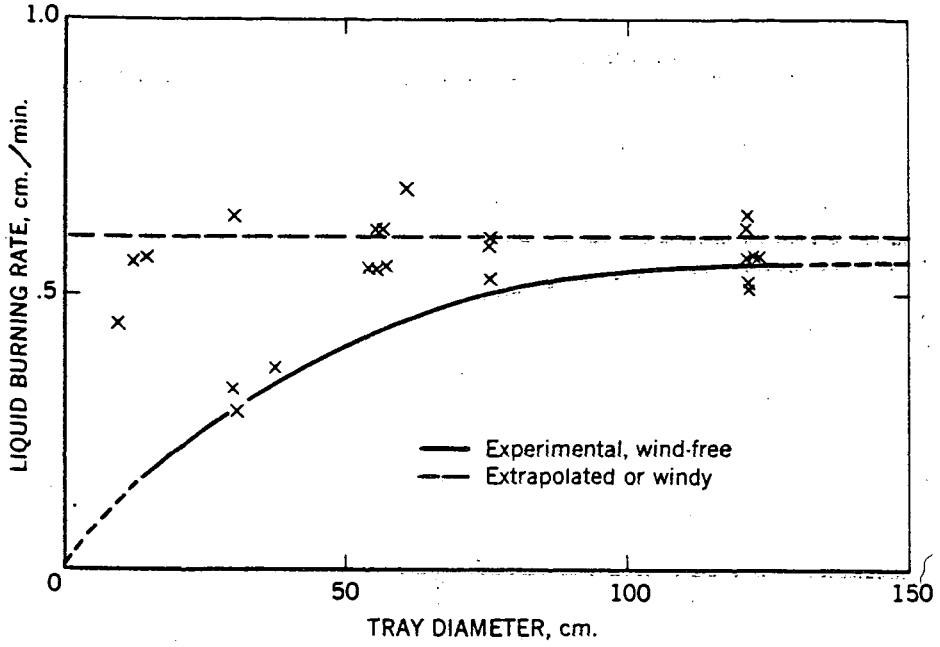


Figure 5.--Effect of Wind on Burning Rate of Benzene.

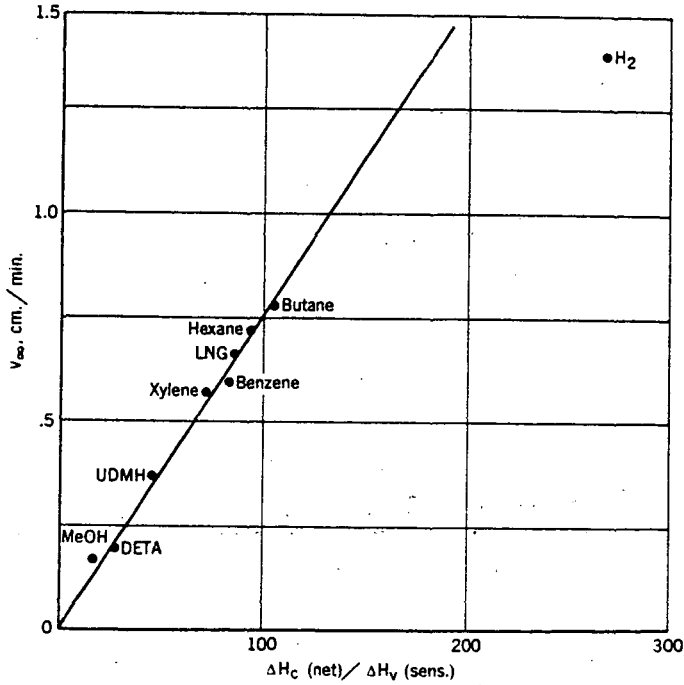


Figure 6.--Relation Between Liquid Burning Rates at Large Pool Diameter and Thermochemical Properties of the Fuels.

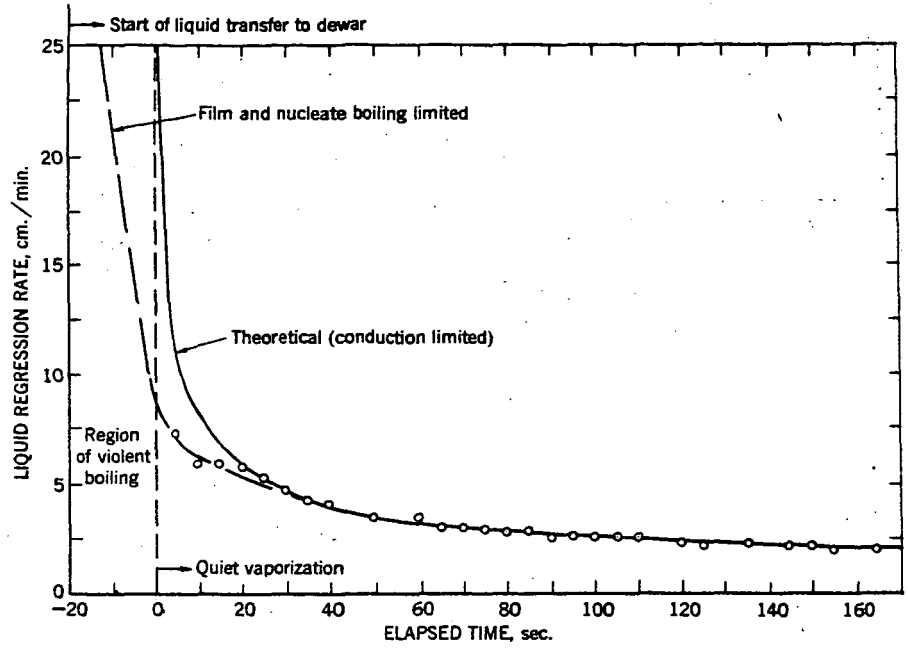


Figure 7.--Rate of Vaporization of Liquid Hydrogen from Paraffin in a 2.8-inch Dewar. Initial liquid depth 6.7 inches.

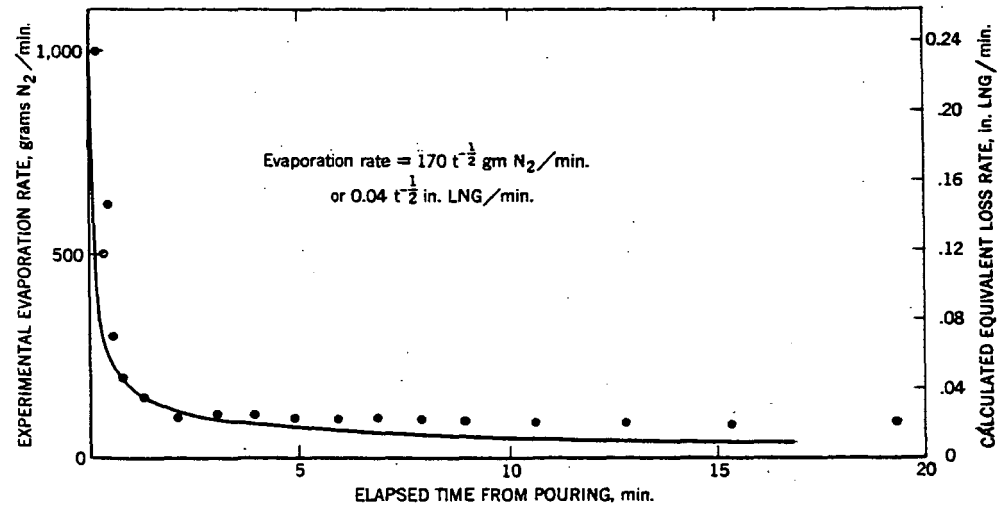


Figure 8.--Evaporation of Liquid Nitrogen after Spillage into a Warm 15-inch Diameter Tray.

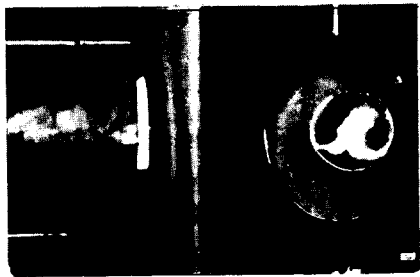
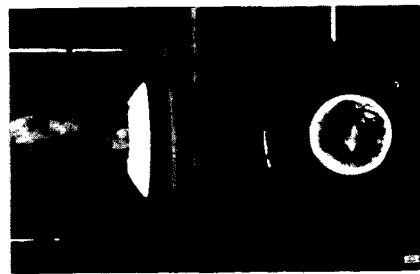
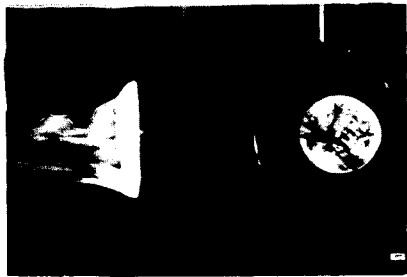


Figure 10.--Side Views and Under Views of Benzene Flames in 6-inch Diameter Dish.

- (a) Flame Undisturbed.
- (b) Radial Draft Induced by Chimney.
- (c) Flame Torn from Rim of Tray.

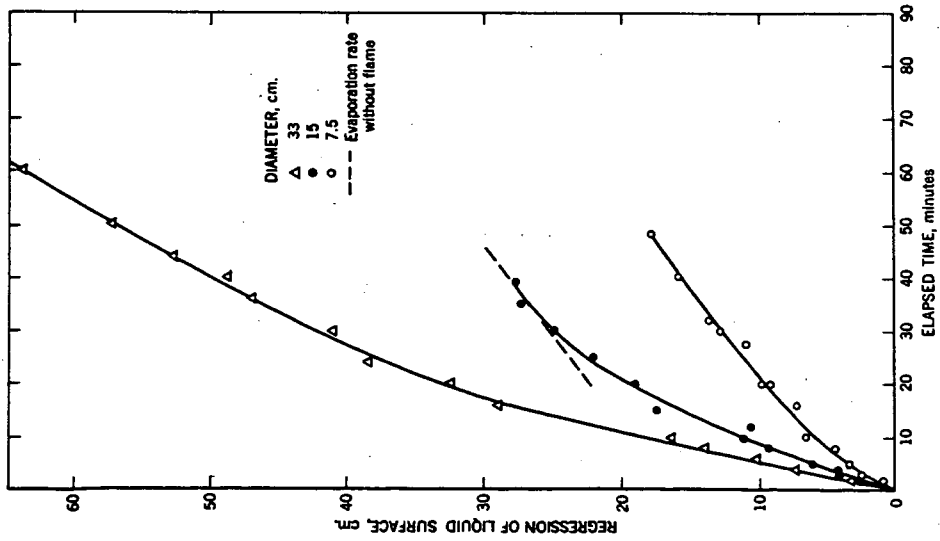


Figure 9.--Burning of Liquid Hydrogen in Stainless Steel Dewars of Three Diameters (reconstructed from flame radiation data, three thermopiles).



0 ————— 5
Scale, inches



Figure 11.--Creeping Flame on Lipless Dish (below)
Compared with Noncreeping Flame on
Dish with 1/2-inch Lip.